Excitonic energy transfer in Au-doped and undoped Kr solids

B. Herkert, A. Schrimpf, K. Göttsche, T. Bornemann, and H.-J. Stöckmann
Fachbereich Physik der Philipps–Universität Marburg and Wissenschaftliches Zentrum für Materialwissenschaften, Renthof 5, D-35032 Marburg, Germany
(Received 23 November 1994)

Excitation of Au-doped krypton solids with synchrotron radiation in the range of the krypton excitons leads to the emission of the molecular self-trapped exciton at 8.41 eV and to a characteristic Au-atom fluorescence at 2.74 eV. By measuring simultaneously the fluorescence-yield spectra of these two emissions and their dependence on parameters such as sample thickness and temperature, crystal quality, and Au concentration, information on the excitonic energy transfer is obtained. An exciton diffusion model describes the measured spectra quantitatively. Exciton diffusion lengths, diffusion constants, and the trapping rate at the Au atoms are evaluated from the data.

I. INTRODUCTION

Excitonic energy transfer in condensed rare gases is a well-known phenomenon, for a review see Ref. 1. A rather unspecific way to produce excitons is x-ray irradiation. In some experiments of this type doped rare gas solids have been irradiated with x rays and the fluorescence of the dopants has been investigated.[2,3] The x rays are absorbed in the solid via a photoeffect resulting in the production of high energy photoelectrons. Then the photoelectrons dissipate their energy by producing a lot of excitons which are partly trapped at the impurities and give rise to their respective fluorescence. In these experiments the concentration of the dopants was too small to account for the high emission intensity by a *direct* absorption of the x rays at the dopants.

A more specific way to study excitonic energy transfer processes is the selective excitation of excitons by resonance absorption. Because of the large band gaps of the rare gas solids the energies of the exciton bands are in the VUV spectral range from about 8.4 eV (Xe) to about 21.3 eV (Ne); therefore it is necessary to use a synchrotron as a light source. During irradiation with synchrotron light in the excitonic range Ophir *et al.* observed the emission of photoelectrons of doped Ar, Kr, and Xe samples due to impurity ionization[4,5] and of undoped solid Xe due to an energy transfer to the Au substrate.[6] In both cases they were able to explain quantitatively their measurements assuming an energy transfer via a diffusion of excitons.

The competing processes to exciton trapping at impurities are direct radiative recombination as well as self-trapping in the solid leading to free exciton (FE) emission or atomic or molecular self-trapped exciton (ASTE, MSTE) emissions, respectively.[7–9] In samples slowly grown from the gas phase close to the triple point Varding *et al.* found a total fluorescence intensity ratio of the FE emission to the emission of the self-trapped centers of about 1 for solid Xe and of about 0.1 in the case of solid Kr.[10] In polycrystalline samples of Kr and Xe, on the other hand, prepared as described in Sec. II, self-trapping into molecular centers is the dominating process and the total fluorescence intensity of the MSTE emission is 2–3 orders of magnitude higher than the intensity of the FE emission.[7,11,12] Ackermann *et al.* measured the fluorescence yield spectra of the MSTE emission in undoped polycrystalline krypton in the range of the Kr excitons.[13] They observed a change with time in the spectra due to a growing layer of residual gas molecules on top of the Kr solids. The energy transfer to impurities at the surface of the crystals was analyzed with the help of an exciton diffusion model as well as with a static energy transfer model, where the dipole-dipole interaction between self-trapped excitons and surface impurities was assumed as a transfer mechanism (the so-called Förster-Dexter mechanism). Unfortunately Ackermann *et al.* were not able to discriminate between the two models.

The ionization of Xe atoms in Ar matrices during exciton excitation detected via photoemission[14] demonstrated that self-trapped excitons were not responsible for the energy transfer; the energy of the MSTE excitons is not sufficient for this ionization. A detailed analysis of the energy distribution curves revealed that the energy transfer took place in the originally excited free-exciton states before self-trapping. With the same technique as applied in Ref. 6, Schwentner *et al.* investigated the energy transfer via excitons from a Kr sample to the Au substrate using photoelectron spectroscopy.[15] The most important result of their work is that the transfer range increases with increasing energy. A small contribution to the transfer via a static transfer mechanism between self-trapped excitons and the substrate could not be excluded, but the significant energy dependence could only be explained by diffusion of free excitons prior to self-trapping.

Stimulated by these works we started a photoluminescence study on energy transfer via excitons in doped and undoped rare gas solids. In Ref. 16 we concentrated on the *trapping process* of excitons at Ag and Au impurities in Ar and Kr solids, while in the present work we report on our measurements of the *transfer process* in undoped and Au-doped krypton. With the help of an exciton diffusion model we are able to extract exciton

0163-1829/95/51(22)/15763(8)/$06.00

diffusion lengths, diffusion constants, and the impurity trapping rate from the data. Some of the results have been published in Ref. 17.

II. EXPERIMENT

The experiments were performed with an UHV matrix isolation apparatus at the Berlin synchrotron radiation facility BESSY. The basic experimental setup was the same as described earlier,[16,18,19] therefore only the essential points and some new features are mentioned here. The samples were prepared by cocondensation of the metal vapor from a Knudsen cell and of the matrix gas onto a cold LiF substrate, cooled by either a closed-cycle cryostat (APD CSA-202, minimal temperature 14 K) or a continuous flow cryostat (modified Oxford CF 1100 UHV, minimal temperature 5 K). Temperatures were measured with calibrated carbon resistors at the sample holders. We obtained a residual gas pressure of 10^{-8} mbar which decreased to 10^{-9} mbar upon cooling down of the cryostat. The sample preparation temperature was varied between 5 K and 30 K. The rare gas pressure during preparation was about 10^{-4} mbar. The deposition rate of the rare gas atoms was determined interferometrically with a HeNe laser and that of the metal atoms was monitored on line with an oscillator microbalance. The metal to rare gas ratio varied between 10^{-5} and 10^{-2} and typical thicknesses ranged from 1 to 3 μm. It is generally accepted that vacuum sublimated rare gas films, like the ones prepared with the setup described above, have a polycrystalline structure (see, e.g., Ref. 20). Quite recently it has been suggested that such samples are better described as nanocrystals.[21,22] Nevertheless our experiments have shown unambiguously that the crystalline areas of our samples are sufficiently extended to exhibit solid state properties like excitons, band structure, and so on. From cluster studies it is known that in clusters with diameters of more than about 5 nm (3000 atoms) the exciton properties are the same as in solids.[23]

The synchrotron light from the storage ring was monochromatized with the 1-m Seya monochromator, covering an energy range from 5 eV to 45 eV with a 600 l/mm grating and a blaze at about 16 eV. The transmitted light was detected with a bialkali photomultiplier with a MgF_2 window (Hamamatsu R292); for such measurements the upper limit of the wavelength range of about 11.3 eV was due to the cutoff of the LiF sample substrate. For preparation the sample had to be turned toward the Knudsen cell. After preparation it was turned back to the incoming synchrotron light to use the full wavelength range of the synchrotron monochromator. Two different detection systems were available for fluorescence measurements. In the visible and the UV ranges the emitted light was collected by a MgF_2 lens in a forward direction at an angle of 30° to the excitation beam. The light was focused through a MgF_2 window onto the entrance slit of a 25 cm crossed Czerny-Turner monochromator. An intensified optical diode array detector (model 1461, EG&G) was hooked onto the exit of the monochromator. With a 150 l/mm grating blazed at 450 nm (2.75 eV) and a 100 μm entrance slit we were able to detect the fluorescence simultaneously in a range of about 450 nm between 180 nm (6.9 eV) and 800 nm (1.55 eV) with a resolution of 2 nm. In the VUV range between 6.2 eV and 11.3 eV the emitted light was collected in a backward direction at an angle of 70° to the incident light by a MgF_2 lens and focused through a MgF_2 window to the entrance slit of a 0.3 m monochromator (McPherson model 218), which was evacuated with a turbomolecular pump to a residual gas pressure below 10^{-5} mbar. The 600 l/mm Al/MgF_2 grating was blazed at 8.3 eV. A solar blind multiplier with a MgF_2 window (Hamamatsu R1459) was used as a detector. To get a good signal-to-noise ratio for fluorescence yield spectra of the MSTE emission in a reasonable time of about 15 min the resolution was set between 12 and 24 nm. The fluorescence spectra presented in this work were not corrected for monochromator and detector characteristics, the fluorescence yield spectra, however, were corrected for intensity and energy dependence of the incident synchrotron light.

III. FLUORESCENCE AND FLUORESCENCE YIELD SPECTRA

Excitation of a Au-doped Kr sample in the range of the Kr excitons leads to a Au emission at 2.74 eV and to the emission of the molecular self-trapped exciton at 8.41 eV (Fig. 1). Au atoms embedded in a rare gas solid show only a characteristic narrow emission (left side of Fig. 1) from the inner shell level $(5d^9 6s^2)^2D_{3/2}$ to the ground state $(5d^{10}6s)^2S_{1/2}$ independent of the excitation in resonant, inner shell or exciton levels.[16,24] For the present purpose it is only important that we have an easily detectable emission to clearly identify the trap-

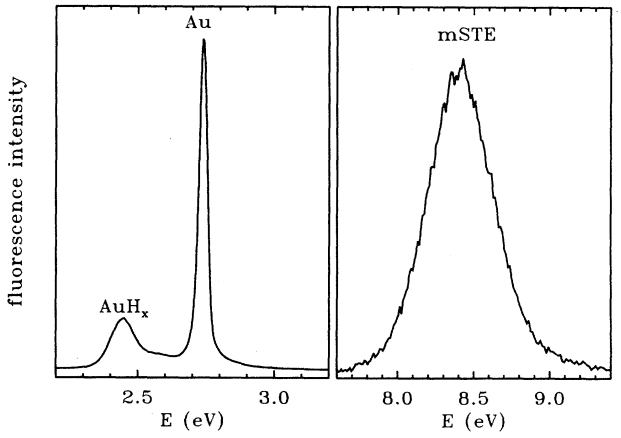

FIG. 1. Emission of the Au atom at 2.74 eV ($^2D_{3/2} \rightarrow {}^2S_{1/2}$) and of an impurity, most probably an AuH complex (left), as well as the emission of the molecular self-trapped exciton at 8.41 eV (right) during exciton excitation at 10.5 eV (preparation temperature T_P = 17 K, measuring temperature T = 15 K, Au concentration $c_0 = 10^{-3}$, sample thickness d = 1080 nm). The sample was not annealed.

ping of excitons at the Au atom. During exciton excitation an additional emission at 2.45 eV is seen (left side of Fig. 1), which was tentatively assigned to a Au-hydrogen complex.[16] In a recent publication on matrix-isolated Au clusters Harbich *et al.* assigned an emission at this energy to a Au_3 cluster.[25] On the right-hand side of Fig. 1 the MSTE emission is shown. We did not observe a free-exciton emission and we did not expect so in view of the polycrystalline samples.

The occurrence of the impurity emissions during exciton excitation demonstrates unambiguously an energy transfer via excitons from the solid to the embedded atoms. In order to get more information about the range and the dynamics of the energy transfer we simultaneously measured the fluorescence yield spectra of the Au and the MSTE emission shown in Fig. 1 in the range of the Kr excitons in dependence on sample thickness, temperature, preparation conditions, and Au concentration.

In Fig. 2 fluorescence yield spectra of the MSTE and the Au emission are shown together with the absorption coefficient of krypton taken from Ref. 26. At first sight one notices the deep minima in the yield spectra at the exciton absorption maxima. This well-known effect[13] is typical for samples which are thick compared to the inverse of the absorption coefficient. The very high absorption coefficient, up to 0.25 nm^{-1}, is correlated via the Kramers-Kronig relation to a high reflection coefficient of up to 50%. Therefore at the maxima of the absorption the light penetrates only a thin layer of the sample and about half of the incident intensity is reflected. At the wings of the absorption peaks the penetration depth is higher and less light is reflected and so the totally absorbed intensity is higher than at the absorption maxima. Both of the yield spectra (lower part of Fig. 2) are modulated with the excitonic structure, a comparison of the two spectra, however, shows that the lower energetic excitons predominantly are self-trapped (the spectrum in the middle of Fig. 2) while the higher energetic excitons are mainly trapped at the Au atoms (the lower spectrum of Fig. 2). This is a clear indication for an energy dependent transfer range.

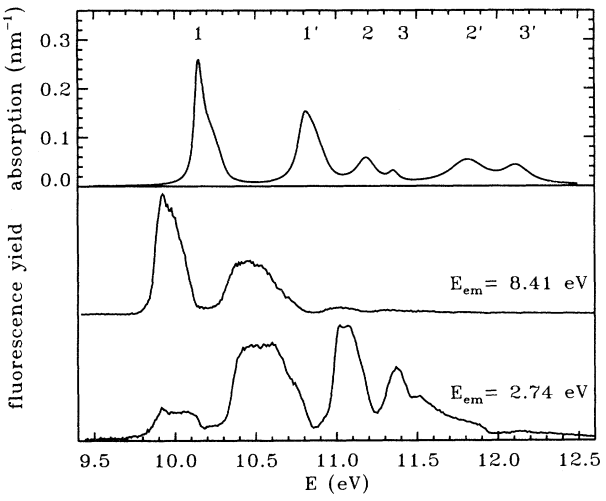

FIG. 2. Fluorescence yield spectra of the MSTE emission at 8.41 eV and of the Au emission at 2.74 eV (bottom). Sample parameters are the same as in Fig. 1. For comparison the absorption coefficient of krypton taken from Ref. 26 is shown in the upper part. The Kr excitons are marked at the top.

The yield spectrum of the Au emission is not impurity specific. Ag- or Cu-doped Kr solids essentially show the same yield spectra of the impurity emissions. Also spectra from literature do not differ much either (e.g., of benzene-doped Kr solids[27]). This shows that the yield spectra are determined by the energy transfer process and not by the impurities.

IV. THE MODEL

The significant energy dependence of our yield spectra and the difference between the Au and the MSTE spectra obviously show that the excitons remember their primarily excited states during the transfer process. This cannot be explained by an energy independent Förster-Dexter mechanism between the self-trapped exciton and the dopants. Therefore we used an exciton diffusion model for the analysis of our data similar to what was used by other authors.[4–6,13,15,28] The energy transfer by means of exciton diffusion can be modeled by the following system of differential equations:

$$\dot{n} = I_0(1-R)\mu e^{-\mu x} + D\frac{d^2n}{dx^2} - \frac{n}{\tau_0} - Sn(c_0 - c_e), \tag{1a}$$

$$\dot{c}_e = Sn(c_0 - c_e) - \frac{c_e}{\tau_c}, \tag{1b}$$

$$\dot{n}_{\mathrm{ST}} = n\left(\frac{1}{\tau_0} - \frac{1}{\tau_r}\right) - \frac{n_{\mathrm{ST}}}{\tau_{\mathrm{ST}}}, \tag{1c}$$

with $n(x,t)$, free-exciton density at time t and at distance x from the surface; $I_0(E)$, number of incident photons per area and time; $\mu(E)$, absorption coefficient; $R(E)$, reflection coefficient; D, diffusion constant; τ_0, lifetime of free excitons with respect to self-trapping and direct recombination; S, trapping rate at the Au atoms; c_0, Au concentration; c_e, concentration of excited Au atoms; τ_c, lifetime of the excited state of the Au atoms; n_{ST}, density of the self-trapped excitons; τ_{ST}, radiative lifetime of self-trapped excitons; and τ_r, radiative lifetime of free excitons.

The change of the free-exciton density $n(x,t)$ with time can be described by four contributions [Eq. (1a)]: creation of excitons by irradiation with light, diffusion, annihilation of free excitons both by radiative recombination and self-trapping, and annihilation by trapping at impurity atoms in their ground state. The concentration of excited Au atoms c_e [Eq. (1b)] increases with trapping of excitons and decreases with radiative recombination. The density of the self-trapped excitons n_{ST} [Eq. (1c)] increases with self-trapping and decreases with the radiative recombination. As we did not observe a free exciton luminescence (see Sec. III), the radiative recombination of free excitons was negligible compared to the

self-trapping ($1/\tau_0 \gg 1/\tau_r$). Second, the total Au atom concentration was large compared to the concentration of the excited Au atoms, i.e., $c_0 \gg c_e$. This was verified by a series of fluorescence yield spectra varying the incident photon flux. We did not observe any saturation effects in the yield spectra. With these approximations Eqs. (1) simplify as follows:

$$\dot{n} = I_0(1-R)\mu e^{-\mu x} + D\frac{d^2n}{dx^2} - \frac{n}{\tau}, \tag{2a}$$

$$\dot{c}_e = Snc_0 - \frac{c_e}{\tau_c}, \tag{2b}$$

$$\dot{n}_{\mathrm{ST}} = \frac{n}{\tau_0} - \frac{n_{\mathrm{ST}}}{\tau_{\mathrm{ST}}}, \tag{2c}$$

where the inverse of the effective lifetime τ of the excitons limited by self-trapping and by trapping at the Au atoms is given by

$$\frac{1}{\tau} = \frac{1}{\tau_0} + Sc_0. \tag{3}$$

Under steady-state conditions corresponding to continuous light irradiation the differential equations (2) can easily be solved. We obtain, for the solution of Eq. (2a),

$$n(x) = \alpha\left(e^{-\mu x} + C_1\cosh(\lambda x) + C_2\cosh(\lambda x)\right) \tag{4}$$

with $\alpha = I_0(1-R)\mu\lambda^2\tau/(\lambda^2-\mu^2)$ and $\lambda = 1/l = 1/\sqrt{D\tau}$. l is the exciton diffusion length, the constants C_1 and C_2 have to be determined from the boundary conditions (see below).

The intensities of the Au and the MSTE emissions, respectively, can now be calculated from Eqs. (2b) and (2c) in dependence on energy, which correspond to the measured yield spectra:

$$I_{\mathrm{MSTE}} = \frac{1}{\tau_{\mathrm{ST}}}\int_0^d n_{\mathrm{ST}}(x)dx = \frac{1}{\tau_0}\int_0^d n(x)dx\ , \tag{5a}$$

$$I_{\mathrm{Au}} = \frac{1}{\tau_c}\int_0^d c_e(x)dx = Sc_0\int_0^d n(x)dx\ . \tag{5b}$$

At both sample interfaces (sample vacuum, $x = 0$, and sample substrate, $x = d$, d denotes the sample thickness) there are two possibilities: either the excitons are reflected into the sample or they are annihilated. In literature always an annihilation at the sample substrate was used. So there are two mathematically different boundary conditions that need to be compared and discussed.

Boundary condition 1: Annihilation at both interfaces,

$$n(0) = 0 \ \text{ and } n(d) = 0.$$

Inserting Eq. (4) into Eq. (2a) we get

$$C_1 = -1,\ C_2 = \frac{\cosh(\lambda d) - e^{-\mu d}}{\sinh(\lambda d)},$$

and

$$\int_0^d n(x)dx = \frac{\alpha}{\mu}\left(1-e^{-\mu d}\right) + \alpha\frac{\left(e^{-\mu d}+1\right)\left[1-\cosh(\lambda d)\right]}{\lambda\sinh(\lambda d)}. \tag{6a}$$

Boundary condition 2: Reflection at the sample-vacuum interface and annihilation at the sample-substrate interface,

$$n'(0) = \left.\frac{dn}{dx}\right|_{x=0} = 0 \ \text{ and } n(d) = 0.$$

Inserting Eq. (4) into Eq. (2a) this time we get

$$C_1 = -\frac{e^{-\mu d}}{\cosh(\lambda d)} - \frac{\mu\sinh(\lambda d)}{\lambda\cosh(\lambda d)},\ C_2 = \frac{\mu}{\lambda},$$

and

$$\int_0^d n(x)dx = \frac{\alpha}{\mu}\left(1-e^{-\mu d}\right) - \alpha\frac{e^{-\mu d}\sinh(\lambda d) + \frac{\mu}{\lambda}\left[\cosh(\lambda d)-1\right]}{\lambda\cosh(\lambda d)}. \tag{6b}$$

With these solutions it was possible to calculate the yield spectra. As we were not able to measure the absorption μ and the reflection R of our samples, we used data from literature.[26]

To decide which boundary condition would be better suited to describe the measured yield spectra, an approximation of expressions (6a) and (6b) is very useful. For a typical thickness of our samples of 1–3 μm one can easily see that in the maxima of the absorption coefficient the approximation $\mu d \gg 1$ holds; and, for an exciton diffusion length l of several ten nanometers, the approximation $\lambda d = d/l \gg 1$ is valid, too. Applying these approximations, the intensity of the MSTE emission can be written in very simple forms.

Boundary condition 1:

$$I_{\mathrm{MSTE}} = \frac{(1-R)\lambda}{\lambda+\mu} = \frac{1-R}{1+\mu l}\ . \tag{7a}$$

Boundary condition 2:

$$I_{\mathrm{MSTE}} = 1 - R. \tag{7b}$$

Equations (7a) and (7b) are valid at the peaks of the Kr absorption spectrum, only, i.e., at the minima of the yield MSTE spectra (such as the curve in the middle of Fig. 2). The solution using boundary condition 2 does not depend on the diffusion length l; for a maximum reflectivity of about 50% it gives a minimum intensity of 50%, which is not in accordance with our data. Using boundary condition 1 the intensity decreases with increasing diffusion length, as now an enhanced number of excitons reaches the sample-vacuum interface and is annihilated there. By choosing an appropriate diffusion length it is therefore possible to fit the solution with boundary condition 1 to our data. *A reflection at the surface (boundary condition 2) is definitely not compatible with our measurements.*

The choice of the boundary condition varies from publication to publication. Ophir *et al.* chose boundary condition 1 (Refs. 4–6) while Schwentner *et al.* had to use boundary condition 2 for a good fit of their data.[15] Ack-

ermann *et al.* observed a change of their spectra with time. They fitted the spectra taken from freshly prepared samples with boundary condition 2, for a good fit of the spectra measured some hours later they used boundary condition 1.[13] They explained this change in the boundary condition with a growing layer of residual gas molecules onto the surface being responsible for the annihilation of the excitons at the surface. We believe that our vacuum conditions are better than those of Ackermann *et al.*; anyhow, we could not observe any changes of our spectra with time. Recent publications on the desorption of atoms after exciton trapping at the surface confirm the annihilation of excitons at the sample-vacuum interface.[29–32]

V. RESULTS AND DISCUSSION

A. Undoped Kr solids

As a first application of the model we tried to fit the measured thickness dependence of the MSTE yield spectrum of undoped krypton. For this case $\lambda = 1/l$ has to be replaced in Eq. (6a) by $\lambda_0 = 1/l_0$, the diffusion length for undoped Kr ($c_0 = 0$). Apart from an energy independent scaling factor the only free parameter for the fit is l_0.

In a first run we fitted the set of yield spectra shown at the top of Fig. 3 at different fixed energies using the same scaling factor for all fits. For one typical energy the result is shown at the bottom of Fig. 3. By this procedure the exciton diffusion lengths were obtained from individual fits as a function of energy. The results showed clearly that the exciton diffusion length l_0 increases with increasing energy. As a good approximation this increase can be described as a linear function of energy in accordance with the results of Schwentner *et al.*[15]

Knowing the energy dependence of the diffusion length in a second step one single fit was applied to each of the complete spectra shown in the upper part of Fig. 3. Furthermore it was necessary to restrict the fit to the energy range $10.1 \leq E \leq 11.4$ eV. For energies higher than 11.4 eV the used spectra of μ and R have pronounced structures, while our yield spectra do not show structures in this area (see Fig. 2). Therefore a fit at these energies would give bad results. An inclusion of the first excitation peak ($E \leq 10.1$ eV) into the fitted range led to physically unreasonable negative diffusion lengths. For energies below 10.1 eV the diffusion length was fixed at a constant value of

$$l_{\min} = 10 \text{ nm} .$$

This value could be varied between 0 and 20 nm without changing the quality of the fit noticeably. Physically, $l_{\min}$ could be interpreted as the range of a Förster-Dexter transport. A typical value for this range is 2 nm,[13] which is clearly within the bandwidth admitted by the fit. These fit restrictions are solely technical and have only a marginal influence on the results. Thus, the only free parameter is the slope a of the assumed linear dependence between the energy and diffusion length.

Fitting the yield spectra at the top of Fig. 3 with this modified model results in an exciton diffusion length of several hundred nanometers depending on energy. The agreement between measured and simulated spectra is good (not shown here). Our l_0 values surpass those of Ref. 15 by up to a factor of 10, but they depend very sensitively on the preparation conditions of the samples. In well-annealed samples l_0 is up to a factor of 2 higher than in freshly prepared ones. In solids prepared at higher temperatures (about 24 K) l_0 is higher than in samples prepared at lower temperatures (about 5 K). For unannealed samples prepared at 5 K we obtain the shortest exciton diffusion lengths which are only a factor of 3 higher than those of Schwentner *et al.*[15]

In the upper part of Fig. 4 the temperature dependence of the MSTE yield spectrum of undoped Kr is presented. The lower energy excitation maximum remains constant while the excitation maxima at higher energies

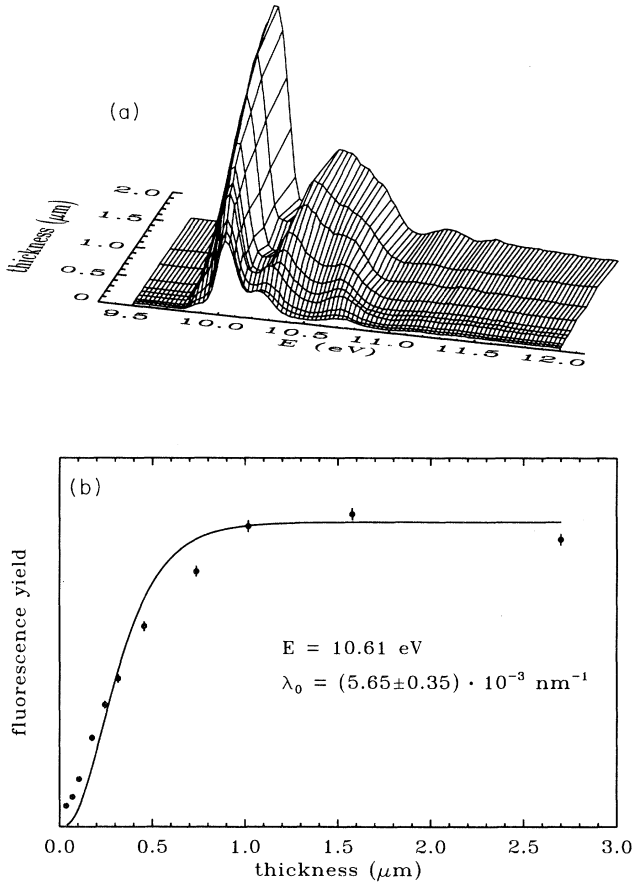

FIG. 3. Top: Measured yield spectra of the MSTE emission at 8.41 eV of undoped krypton in dependence on sample thickness (preparation and measuring temperature $T = 23.6$ K). The sample thickness was varied by successive condensation of Kr layers on top of the existing sample. Bottom: Fit of the exciton diffusion model to the measured thickness dependence of the MSTE intensity at $E = 10.61$ eV (for details see text).

increase with increasing temperature. Obviously, self-trapping of higher energy excitons is enhanced at higher temperatures leading to an increase of the MSTE emission intensity. This enhancement can be understood in terms of a reduction of the exciton diffusion length (lower part of Fig. 4), which means that a smaller part of excitons will be annihilated at the sample surface. This is in accordance with the known decrease of the free-exciton lifetime τ_0 with increasing temperature.[12] The agreement between measured and simulated spectra is very good, we presented the comparison of the measured and simulated temperature dependence in Ref. 17.

To calculate the diffusion constant D from the diffusion length one needs to know the free-exciton lifetime τ_0. Two measurements of the temperature dependence of τ_0 in Kr exist.[10,12] In Ref. 10 exciton lifetimes are reported, which are about 1 order of magnitude longer than the results reported in Ref. 12 due to a much better crystal quality. As the preparation conditions described in Ref. 12 were comparable to ours we used the values given there for the $n = 1$ exciton at 10.2 eV to determine the diffusion constant D from the extracted diffusion lengths for temperatures in the range 8–32 K. Averaging over these results we obtained

$$D = (0.16 \pm 0.02)\ \mathrm{cm^2\,s^{-1}}.$$

This value is at the lower limit of those discussed in literature,[1,7,9] which were derived from estimations or theoretical calculations and are very uncertain.

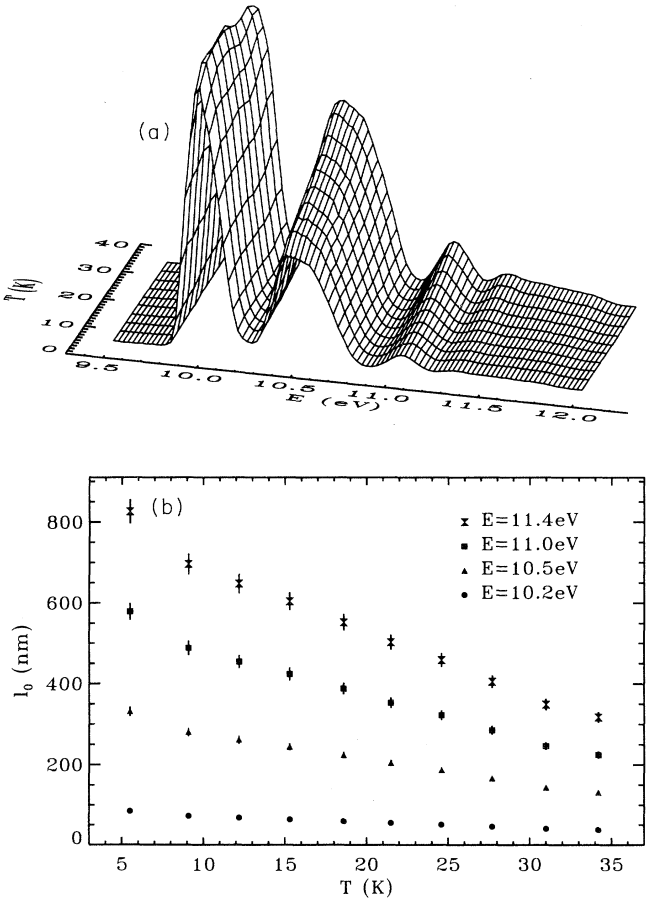

FIG. 4. Top: Measured temperature dependence of the fluorescence yield spectra of the MSTE emission at 8.41 eV in undoped Kr (preparation temperature $T_P = 5.6$ K, sample thickness $d = 2100$ nm). Prior to the measurements the sample was annealed up to 34 K. Bottom: Dependence of the exciton diffusion length l_0 on temperature at four typical energies.

B. Au-doped Kr solids

In Au-doped krypton excitons can be trapped additionally at the Au atoms with the rate S. As our measurements were not time resolved we could only get information about parameter combinations, which do not depend on the time explicitly, such as $\sqrt{D\tau_0}$ or S/D. Using the l_0 values of similarly prepared undoped Kr solids, S/D is the only further parameter in fitting the yield spectra of Au-doped samples. Averaging over the results obtained from fits to the spectra of 20 samples we get

$S/D = (2.1 \pm 1.0) \times 10^{13}\ \mathrm{cm^{-2}}$ for unannealed samples,
$S/D = (0.52 \pm 0.07) \times 10^{13}\ \mathrm{cm^{-2}}$ for annealed samples.

As S can be assumed to be specific for the Au atoms and independent on the crystal quality this difference yields a four times higher diffusion constant for annealed samples. This is in accordance with the above-mentioned dependence of l_0 on the annealing process. Using the derived value for D and taking S/D for annealed samples we obtained for the trapping rate S at the Au atoms

$$S = (0.83 \pm 0.15) \times 10^{12}\ \mathrm{s^{-1}}.$$

This is of the order of the Debye frequency of solid Kr ($\nu_{\mathrm{Debye}} = 1.5 \times 10^{12}\ \mathrm{s^{-1}}$) (Ref. 33) and is in accordance with the picture that the exciton-phonon interaction is responsible for the trapping process.

As an example for measurements on Au-doped samples we present the concentration dependence of the yield spectra. From the definition of the diffusion length $l = \sqrt{D\tau}$ and Eq. (3) one gets

$$\frac{1}{l^2} = \frac{1}{l_0^2} + \frac{S}{D} c_0 \,. \tag{8}$$

Thus, with increasing Au concentration we expect a reduction of the diffusion length l. More and more excitons should be trapped at the Au atoms and the MSTE signal should decrease. In the upper part of Fig. 5 the measured MSTE and Au emission yield spectra are shown in dependence on the Au concentration. The MSTE spectra in Fig. 5 have been normalized to the excitation peak at 10.0 eV while the Au spectra have been normalized to the peak at 11.3 eV.

The maxima of the MSTE yield spectra show a more pronounced decrease with increasing Au concentration the higher the energy. Therefore in the Au yield spectra

one would expect an increase of the lower energy peaks relative to the maximum at 11.3 eV but the measured effect is not significant.

The concentration dependence of the MSTE yield spectra is another evidence for the energy dependence of the transfer range. The excitons with the highest diffusion length, i.e., with the highest energies, are trapped completely at the Au atoms even at small concentrations, whereas for the lower energetic excitons with a smaller transfer range higher concentrations are necessary for impurity trapping. In an extremely highly doped sample ($c_0 \approx 3\%$) we measured a MSTE yield spectrum (not included in Fig. 5), which showed a total quenching of the MSTE emission apart from a very weak excitation peak at 10.0 eV.

The lower part of Fig. 5 shows a simulation of the spectra obtained from Eqs. (6a) and (5a). The agreement of the calculated MSTE spectra (lower left side) with the measured ones (upper left side) is good. The calculation reproduces the characteristic decrease of the excitation peaks with Au concentration at higher energies. For the simulated Au spectra the agreement with the measured ones is only moderate, the relative peak heights are not reproduced very well. The cause for this phenomenon, which is characteristic for all our simulations of the Au spectra, is a rather trivial one and can be traced back to uncertainties in the used spectra of μ and R.[26] Our spectra have a good signal-to-noise ratio at the excitation maxima, whereas the spectra of μ and R are more accurate at the absorption and reflection maxima, i.e., at the excitation minima (see Fig. 2). A small change in the minima of the absorption coefficient would be sufficient to obtain a good agreement between measured and calculated spectra.

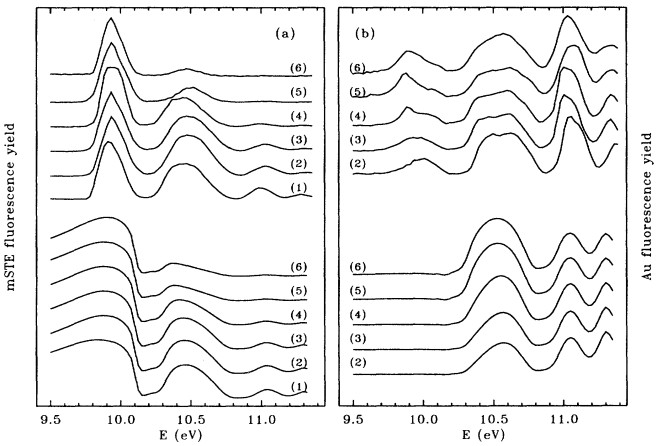

FIG. 5. Top: Measured yield spectra of the MSTE emission at 8.41 eV (a) and of the Au emission at 2.74 eV (b) in dependence on the Au concentration [six different samples, sample thicknesses ranging from 940 nm to 1400 nm, preparation temperatures from 16.2 K to 17.9 K, measuring temperatures about 14 K, Au concentrations c_0 (1) 0, (2) 5.6×10^{-5}, (3) 2.4×10^{-4}, (4) 1.1×10^{-3}, (5) 4.4×10^{-3}, (6) 6.4×10^{-3}]. Prior to the measurements the samples have been annealed up to 35 K. It was impossible to compare the absolute fluorescence intensity. Therefore the MSTE spectra have been normalized to the same intensity at 10.0 eV, the Au spectra at 11.3 eV. Bottom: Simulated yield spectra of the MSTE emission at 8.41 eV (a) and of the Au emission at 2.74 eV (b) in dependence on Au concentration. For the simulation we used $S/D = 0.52 \times 10^{13}$ cm^{-2} and a slope for the increase of the diffusion length with energy of $a = 236$ nm/eV. Below 10.1 eV the simulated spectra do not describe the measurements correctly as the exciton diffusion model can not be applied in that energy range (see Sec. V A).

In analogy to undoped krypton we measured the temperature dependence of the MSTE spectrum of Au-doped samples, too. Using the results for the temperature dependence of the diffusion lengths of undoped Kr and the results for S/D after annealing we could simulate the spectra in very good agreement with the measured ones. A simulation of the temperature dependence of the Au spectra with the model was not possible because of temperature dependent atomic relaxation processes after trapping of excitons into inner shell levels of the Au atoms.[16] The measured dependence of the Au and MSTE spectra on the thickness of a pure Kr layer upon the Au-doped sample could be simulated with the model as well (not shown here).

VI. CONCLUSIONS

With the help of an exciton diffusion model we were able to evaluate diffusion lengths, diffusion constants, and the trapping rate at impurity atoms from our data and thus to explain all our measured spectra in dependence on sample thickness, temperature, and Au concentration. The experiments show unambiguously that the exciton diffusion length l_0 and the diffusion constant D depend very sensitively on the preparation conditions and the crystal quality. This explains the wide range of the results in literature.

We would like to emphasize two important results: first, the increase of the exciton diffusion lengths with energy is responsible for the obvious energy dependent difference between the yield spectra of the MSTE and the Au emission (Fig. 2). Comparing Eqs. (5a) and (5b) one finds that the only energy dependent quantity entering into the yield ratio is the free-exciton lifetime τ_0. Thus, we have to conclude that the energy dependence of the exciton diffusion length $l_0 = \sqrt{D\tau_0}$ is not due to an energy dependence of the diffusion constant but of the lifetime. So far no measurements of the lifetime of higher exciton states exist, but we think it is worth checking our findings by independent lifetime measurements.

A second, somewhat astonishing result is the very large diffusion length, which for higher energetic excitons at low temperatures (see Fig. 4) is on the order of the sample thickness. A diffusion length in the same order of magnitude has been reported recently for solid Xe.[10,34] It is highly questionable whether the used diffusion model gives a correct description of the transport process in this extreme case. An alternative model could be a coherent transport of excitons in their different quantum states combined with a successive relaxation from higher to lower states until they are finally self-trapped or impurity trapped. This is a much more complicated model,

which needs more parameters than the model we used. Time resolved pump-probe experiments in the different higher exciton states should be able to give an answer to this question.

ACKNOWLEDGMENTS

This work was supported by the Bundesministerium für Forschung und Technologie of the Federal Republic of Germany. We would like to thank Professor D. M. Kolb (Universität Ulm) and Dr. W. Schulze (Fritz-Haber-Institut, Berlin) for giving us the opportunity to study our systems with their apparatus at BESSY. U. Schriever, Dr. T. Hebert, R. Brüning, and L. König are thanked for their help during the beamtimes at BESSY. Professor H. Ackermann (Philipps–Universität, Marburg) is thanked for helpful discussions.

[1] N. Schwentner, E.-E. Koch, and J. Jortner, in *Electronic Excitations in Condensed Rare Gases*, Vol. 107 of *Springer Tracts in Modern Physics* (Springer, Berlin, 1985), Chap. 6.
[2] E. Schuberth and M. Creuzburg, Phys. Status Solidi B **90**, 189 (1978).
[3] R. Dersch, B. Herkert, M. Witt, H.-J. Stöckmann, and H. Ackermann, Z. Phys. B. **80**, 39 (1990).
[4] Z. Ophir, B. Raz, and J. Jortner, Phys. Rev. Lett. **33**, 415 (1974).
[5] Z. Ophir, B. Raz, J. Jortner, V. Saile, N. Schwentner, E.E. Koch, M. Skibowski, and W. Steinmann, J. Chem. Phys. **62**, 650 (1975).
[6] Z. Ophir, N. Schwentner, B. Raz, M. Skibowski, and J. Jortner, J. Chem. Phys. **63**, 1072 (1975).
[7] I.Y. Fugol, Adv. Phys. **27**, 1 (1978).
[8] G. Zimmerer, in *Excited State Spectroscopy in Solids*, edited by U.M. Grassano and N. Terzi (North-Holland, Amsterdam, 1987), Chap. 1.
[9] I.Y. Fugol, Adv. Phys. **37**, 1 (1988).
[10] D. Varding, J. Becker, L. Frankenstein, B. Peters, M. Runne, A. Schröder, and G. Zimmerer, Low Temp. Phys. **19**, 427 (1993).
[11] E. Roick, R. Gaethke, G. Zimmerer, and P. Gürtler, Solid State Commun. **47**, 333 (1983).
[12] E. Roick, R. Gaethke, P. Gürtler, and G. Zimmerer, J. Lumin. **31&32**, 102 (1984).
[13] C. Ackermann, R. Brodmann, U. Hahn, A. Suzuki, and G. Zimmerer, Phys. Status Solidi B **74**, 579 (1976).
[14] N. Schwentner and E.E. Koch, Phys. Rev. B **14**, 4687 (1976).
[15] N. Schwentner, G. Martens, and H.W. Rudolf, Phys. Status Solidi B **106**, 183 (1981).
[16] A. Schrimpf, B. Herkert, L. Manceron, U. Schriever, and H.-J. Stöckmann, Phys. Status Solidi B **165**, 469 (1991).
[17] B. Herkert, A. Schrimpf, K. Göttsche, T. Bornemann, R. Brüning, and H.-J. Stöckmann, J. Lumin. **60&61**, 768 (1994).
[18] H. Wiggenhauser, W. Schroeder, and D.M. Kolb, J. Chem. Phys. **88**, 3434 (1988).
[19] T. Hebert, H. Wiggenhauser, and D.M. Kolb, J. Chem. Phys. **91**, 1417 (1989).
[20] J.A. Venables and B.L. Smith, in *Rare Gas Solids*, edited by M.L. Klein and J.A. Venables (Academic, London, 1977), Vol. II, Chap. 10.
[21] N. Steinmetz, H. Menges, J. Dutzi, H.v. Löhneysen, and W. Goldacker, Phys. Rev. B **39**, 2838 (1989).
[22] A. Schrimpf, R. Rosendahl, T. Bornemann, H.-J. Stöckmann, F. Faller, and L. Manceron, J. Chem. Phys. **96**, 7992 (1992).
[23] J. Stapelfeld, J. Wörmer, and T. Möller, Phys. Rev. Lett. **62**, 98 (1989).
[24] W. Schrittenlacher and D.M. Kolb, Ber. Bunsenges. Phys. Chem. **88**, 492 (1984).
[25] W. Harbich, S. Fedrigo, J. Buttet, and D.M. Lindsay, J. Chem. Phys. **96**, 8104 (1992).
[26] I.T. Steinberger, P. Maaskant, and S.E. Webber, J. Chem. Phys. **66**, 4722 (1977).
[27] S.S. Hasnain, T.D.S. Hamilton, I.H. Munro, E. Pantos, and I.T. Steinberger, Philos. Mag. **35**, 1299 (1977).
[28] O. Simpson, Proc. R. Soc. London, Ser. A **238**, 402 (1957).
[29] J.W. Boring, R.E. Johnson, and D.J. O'Shaughnessy, Phys. Rev. B **39**, 2689 (1989).
[30] T. Kloiber and G. Zimmerer, Radiat. Eff. Def. Solids **109**, 219 (1989).
[31] E. Hudel, E. Steinacker, and P. Feulner, Phys. Rev. B **44**, 8972 (1991).
[32] G. Zimmerer, Nucl. Instrum. Methods B **91**, 601 (1994).
[33] P. Korpuin and E. Lüscher, in *Rare Gas Solids* (Ref. 20), Chap. 12.
[34] D. Varding, I. Reimand, and G. Zimmerer, Phys. Status Solidi B **185**, 301 (1994).